Mechanism and regulation of the Two-component FMN-dependent monooxygenase ActVA-ActVB from Streptomyces coelicolor.

Julien Valton, Carole Mathevon, Marc Fontecave, Vincent Nivière, David P Ballou

▶ **To cite this version:**

Julien Valton, Carole Mathevon, Marc Fontecave, Vincent Nivière, David P Ballou. Mechanism and regulation of the Two-component FMN-dependent monooxygenase ActVA-ActVB from Streptomyces coelicolor.. Journal of Biological Chemistry, 2008, 283, pp.10287-96. 10.1074/jbc.M709730200 . hal-01075299

HAL Id: hal-01075299
https://hal.science/hal-01075299

Submitted on 7 Jan 2015

HAL is a multi-disciplinary open access archive for the deposit and dissemination of scientific research documents, whether they are published or not. The documents may come from teaching and research institutions in France or abroad, or from public or private research centers.

L'archive ouverte pluridisciplinaire **HAL**, est destinée au dépôt et à la diffusion de documents scientifiques de niveau recherche, publiés ou non, émanant des établissements d'enseignement et de recherche français ou étrangers, des laboratoires publics ou privés.

THE TWO-COMPONENT FMN-DEPENDENT MONOOXYGENASE ACTVA-ACTVB FROM *STREPTOMYCES COELICOLOR* : MECHANISM AND REGULATION*

Julien Valton[1], Carole Mathevon[2,3,4], Marc Fontecave[2,3,4], Vincent Nivière[2,3,4] and David P. Ballou[1]

[1] Department of Biological Chemistry, University of Michigan, Ann Arbor, MI 48109-0606, USA. [2] CEA, DSV, iRTSV, Laboratoire de Chimie et Biologie des Métaux, 17 Avenue des Martyrs, Grenoble F-38054, France. [3] CNRS, UMR 5249, Grenoble F-38054, France. [4] Université Joseph Fourier, Grenoble F-38000, France.

Running title: Mechanism and regulation of ActVA-ActVB monooxygenase system

Address correspondence to: Vincent Nivière; LCBM-iRTSV, CEA, 17 Avenue des Martyrs, Grenoble F-38054, France, Tel: 33 4 38 78 91 09, Fax: 33 4 38 78 91 24, E. mail: vniviere@cea.fr
David P. Ballou; Dept of Biological Chemistry, University of Michigan, Ann Arbor, MI 48109-0606, USA, Tel: 734 764 9582, Fax: 734 764 3509, E. mail: dballou@umich.edu

The ActVA-ActVB system from *Streptomyces coelicolor* is a two-component flavin-dependent monooxygenase involved in the antibiotic actinorhodin biosynthesis. ActVB is a NADH:flavin oxidoreductase that provides a reduced FMN to ActVA, the monooxygenase that catalyzes the hydroxylation of dihydrokalafungin, the precursor of actinorhodin. In this work, using stopped-flow spectrophotometry, we investigated the mechanism of hydroxylation of dihydrokalafungin catalyzed by ActVA and that of the reduced FMN transfer from ActVB to ActVA. Our results show that the hydroxylation mechanism proceeds with the participation of two different reaction intermediates in ActVA active site. First, a C(4a)-FMN-hydroperoxide species is formed after binding of reduced FMN to the monooxygenase and reaction with O_2. This intermediate hydroxylates the substrate and is transformed to a second reaction intermediate, a C(4a)-FMN-hydroxy species. In addition, we demonstrate that reduced FMN can be transferred efficiently from the reductase to the monooxygenase without involving any protein-protein complexes. The rate of transfer of reduced FMN from ActVB to ActVA was found to be controlled by the release of NAD^+ from ActVB and was strongly affected by NAD^+ concentration, with an IC_{50} of 40 µM. This control of reduced FMN transfer by NAD^+ was associated with the formation of a strong charge-transfer complex between NAD^+ and reduced FMN in the active site of ActVB. These results suggest that in *Streptomyces coelicolor*, the reductase component ActVB can act as a regulatory component of the monooxygenase activity by controlling the transfer of reduced FMN to the monooxygenase.

The flavin dependent monooxygenases are important enzymes that are involved in a wide variety of biological reactions. One of their fundamental functions uses their reduced flavins to activate molecular oxygen by generating flavin-hydroperoxide intermediates, the reactive species that oxygenate the substrate. Two different classes of flavin-dependent monooxygenases have been described. The first class comprises the well-known single-component flavoprotein monooxygenases, in which within a single polypeptide chain, the flavin cofactor is reduced by NAD(P)H and reacts with O_2 to generate the flavin-hydroperoxide species. Some of these flavoproteins have been investigated in great detail, *p*-hydroxybenzoate hydroxylase being the prototype of this class of flavoprotein monooxygenase (*1*). More recently, several two-component flavin-dependent monooxygenases, present in prokaryotic cells and involved in a broad range of oxygenation reactions, have been reported. These systems use two different proteins, a reductase for reducing the flavin and an oxygenase for binding the reduced flavin and

catalyzing the reaction with O_2. Examples of two-component monooxygenases that use reduced FAD (FAD_{red}) as a cofactor are 4-hydroxyphenylacetate monooxygenase (HpaB) from *Escherichia coli* (*2*), phenol hydroxylase (PheA1) from *Bacillus thermoglucosidaflurescens* (*3*) and styrene monooxygenase (StyA) from *Pseudomonas fluorescens* (*4, 5*). Two-component flavin-dependent monooxygenases that use reduced FMN (FMN_{red}) include enzymes involved in the biosynthesis of the antibiotic pristinamycin in *Streptomyces pristinaespiralis* (*6, 7*), in the utilization of sulfur from aliphatic sulfonates in *Escherichia coli* (*8*) and in the desulfurization of fossil fuels by *Rhodococcus* species (*9*), as well as the hydroxylation of 4-hydroxyphenylacetate in *Acinetobacter baumannii* (*10*). We have been investigating the mechanism of the FMN-dependent two-component enzyme system, ActVA-ActVB, which participates in the last steps of the biosynthesis of the antibiotic actinorhodin in *Streptomyces coelicolor* (*11-13*) (Scheme 1).

The first enzyme of the two-component flavin-dependent oxygenases is a NAD(P)H:flavin oxidoreductase that catalyzes the reduction of free oxidized flavins (FAD and/or FMN) by the reduced pyridine nucleotides, NADPH or NADH (*3, 14-16*). The second enzyme is an oxygenase that binds the resulting free reduced flavin and promotes its reaction with O_2 to hydroxylate the substrate (*2, 3, 5-10, 17*). Therefore, in contrast to the single-component flavin hydroxylases, the two-component systems catalyze the reduction of the flavin and the hydroxylation of the substrate on separate polypeptides. In the biosynthesis of actinorhodin the hydroxylase system consists of the reductase, ActVB, and the oxygenase, ActVA (*14,15,17*). There is now general agreement that the hydroxylation steps of flavin-dependent hydroxylases proceed through the reaction of the reduced flavin with molecular oxygen to generate a flavin C(4a)-hydroperoxide intermediate (*18*). This is followed by the transfer of an oxygen atom from the peroxide to the substrate.

Catalysis by the two-component flavin-dependent monooxygenases requires that the reduced flavin be transferred from the reductase to the monooxygenase without being oxidized by molecular O_2. This would appear to be a very challenging process because free reduced flavin becomes oxidized quite rapidly in the presence of O_2. Such an oxidation must be avoided or the reduction of the flavin and the ensuing hydroxylation reaction would effectively be uncoupled and, instead, NAD(P)H would be consumed to produce H_2O_2 and superoxide. We have previously demonstrated that with the ActVA-ActVB system from *S. coelicolor* the transfer of FMN_{red} from the reductase to the oxygenase is thermodynamically favorable (*17*). Indeed the monooxygenase ActVA binds FMN_{red} with a K_d value of 0.39 μM and FMN_{ox} with a K_d value of about 20 μM, while the reductase ActVB binds FMN_{ox} more tightly than $FMN_{red.}$ There is also no evidence for specific binding interactions between the two components that might facilitate a channeling mechanism allowing the flavin to travel from one protein to another within a protein complex. These data suggest that in spite of the drawbacks associated with the simultaneous presence of free FMN_{red} and O_2, FMN_{red} is probably transferred between the two components by diffusion and rapid binding to the oxygenase during the hydroxylation reaction.

In this work, we have determined that FMN_{red} can be transferred very efficiently from the reductase to the monooxygenase without the participation of any protein-protein complexes. In addition, our data show that in the *S. coelicolor* system the rate of transfer of FMN_{red} from the reductase, ActVB to the hydroxylase, ActVA, is controlled by the release of NAD^+ from ActVB, and that the concentration of NAD^+ strongly affects this rate. This is manifest by the formation of a strong charge-transfer complex between NAD^+ and FMN_{red} in the active site of ActVB.

EXPERIMENTAL PROCEDURES

Materials. NAD^+, NADH, and FAD were from Sigma. FMN was prepared by conversion of FAD to FMN with snake venom from *Crotalus adamanteus* (*19*). DCPIP and menadione were from Sigma. 5-Deazaflavin (5-deaza-5-carba-riboflavin) was a gift from Dr. Philippe Simon (Grenoble, France). Enantiopure (+)-Kalafungin was synthesized by Dr. Rodney Fernandes and provided by Prof. Dr. Reinhard. Brückner (Freiburg, Germany) (*20*). DHK (dihydrokalafungin), the non-lactonic analogue of (+)-kalafungin, was obtained from the reductive treatment of (+)-kalafungin by $NaBH_4$ as described in (*21*). A

solution containing 40 µM (+)-kalafungin in anaerobic 50 mM Tris-HCl buffer, pH 7.4, was mixed with ~7 equivalents of $NaBH_4$. The reaction was allowed to proceed for a few seconds under anaerobic conditions and the mixture was then opened to air. The formation of DHK was verified by UV-visible spectrophotometry and LC-MS/MS. Both techniques showed that (+)-kalafungin was efficiently transformed to DHK with a yield of ~100 % (data not shown). HPAH-C_2 from *A. baumanii* was provided by Dr. Jeerus Sucharitakul (Mahidol University, Thailand). Recombinant ActVA-Orf5 and His-tagged ActVB from *S. coelicolor* were overexpressed in *E. coli* and purified as described previously (*14, 17*).

Anaerobic procedures and rapid reaction experiments. All reactions were performed in 50 mM Tris-HCl buffer, pH 7.4, at 4°C. Solutions were made anaerobic in glass tonometers by ~20 cycles of vacuum and equilibration with Ar_2 gas that was depleted from oxygen contamination with an Oxiclear oxygen removal column (Labclear) as described previously (*22*). To minimize oxygen contamination of reaction mixtures due to diffusion through valves, etc, all anaerobic solutions contained an oxygen-scrubbing solution consisting in 12.5 to 25 µM protocatechuate (PCA, final concentrations) and ~0.06 units/ml of protocatechuate dioxygenase (PCD, final concentration). This mixture has been shown to maintain anaerobic conditions efficiently (*23*).

Rapid kinetics reactions were performed with a Hi-Tech Scientific stopped-flow Model SF-61DX instrument operating either in single or in double mixing mode, and using either a diode array spectrophotometer or a photomultiplier detector. Kinetic traces were analysed and fitted with KinetAsyst 3 software (Hi-Tech Scientific, Salisbury, UK). Before each experiment, the stopped-flow instrument flow system was made anaerobic by incubating the flow system overnight with an oxygen scrubbing solution consisting of 100 mM PCA and 0.06 units/ml PCD in potassium phosphate buffer, pH 7.

Reaction of ActVA·FMN_{red} with O_2 in the presence or in the absence of the pyronaphthoquinone substrate DHK_{red}. A solution containing ActVA (50 µM), FMN_{ox} (20 µM), deazaflavin (60 nM), EDTA (10 mM) and catalase (50 nM) in 50 mM Tris-HCl buffer, pH 7.4, was made anaerobic in a glass tonometer as described above. FMN_{ox} was then photoreduced for 5 to 10 sec using a commercial 1000 W tungsten-halogen lamp placed ~10 cm away from the solution. The redox status of FMN was monitored by UV-visible spectrophotometry. When experiments were performed in the presence of DHK, the same reaction mixture as indicated above was used, but included the presence of 80 µM DHK. Both FMN_{ox} and oxidized DHK (DHK_{ox}) were photoreduced together by the procedure described above. This solution was then mixed in the stopped-flow instrument with an equal volume of a solution containing various concentrations of oxygen, and the reaction was followed spectrophotometrically at various wavelengths, or by spectrofluorimetry with excitation at 390 nm and emission at wavelengths > 530 nm. Oxygenated solutions were prepared by equilibrating 50 mM Tris-HCl buffer for 30 min with air (21% oxygen) or with certified oxygen/nitrogen gas mixtures (5, 10, 50, 100 % oxygen).

Investigation of the kinetics of FMN_{red} transfer. To study the transfer of FMN_{red} from ActVB to the monooxygenase (ActVA or HPAH-C_2), the ActVB·FMN_{red} complex was prepared. A solution containing ActVB (85 µM) and FMN_{ox} (20 µM) in Tris-HCl buffer, pH 7.4, in a glass tonometer equipped with a cuvette was made anaerobic as described above. The excess ActVB was to assure that most of the FMN was bound. The complex was then reduced by titration with an anaerobic solution of NADH delivered by a gastight Hamilton syringe connected to the tonometer via an Airless Ware fitting. Approximately 20 µM of NADH was sufficient to fully reduce the ActVB·FMN complex. This complex was then mixed in the stopped-flow instrument with an equal volume of Tris-HCl buffer containing ActVA (45 µM) and O_2 (600 µM), HPAH-C_2 from *A. baumanii* (45 µM) and O_2 (600 µM), oxidized DCPIP (2,6-dichlorophenolindophenol, 20 µM), or oxidized menadione (40 µM). The concentrations given are those in the syringes before mixing. The inhibition of FMN_{red} transfer from ActVB to HPAH-C_2 by NAD^+ was investigated by a double mixing stopped-flow technique. The ActVB·FMN_{red}·NAD^+ complex prepared as described above (235, 40

and 40 μM of each component respectively), was first mixed into an aging chamber with a solution containing various concentrations of NAD^+ (from 0 to 5 mM). After a 5 s delay to assure that the binding of NAD^+ had come to equilibrium, the solution from the first mix was mixed with an equal volume of 50 mM Tris-HCl buffer containing HPAH-C_2 (50 μM) and O_2 (255 μM), and the FMN_{red} transfer to HPAH-C_2 was followed spectrophotometrically at 386 and 700 nm to observe the formation of the C(4a)-FMN-OOH intermediate and the disappearance of the FMN_{red}–to–NAD^+ charge-transfer complex.

RESULTS

Reaction of ActVA-FMN_{red} with O_2 in the absence of the pyronaphthoquinone substrate. Formation and decay of the C(4a)-FMN-OOH intermediate. It has been previously shown that ActVA is able to stabilize a C(4a)-FMN-OOH species within its active site, but the kinetics of its formation and decay were not determined (*17, 24*). Here, we have investigated the kinetics of the formation and decay of the C(4a)-FMN-OOH intermediate by stopped-flow spectrophotometry at 4°C, as described in Materials and Methods. An anaerobic solution of FMN_{red} (20 μM), containing an excess of ActVA (50 μM) to promote full complex formation ($K_{d\ FMNred}$ = 0.39 μM, (*17*)), was mixed with equal volumes of Tris-HCl buffer solution containing various concentrations of O_2. The reaction was monitored by UV-visible spectrophotometry. As shown in Fig. 1*A* (thick line) the first spectrum recorded at 5 s ($[O_2]$ = 595 μM after mixing) has a main absorption band at 386 nm. This spectrum is characteristic of a C(4a)-FMN-OOH species, such as those found in other single- and two-component flavin-dependent hydroxylases, including 4-hydroxyphenylacetate 3-hydroxylase (HPAH-C_2) from *A. baumannii* (*22*) and *p*-hydroxybenzoate hydroxylase (PHBH) from *Pseudomonas aeruginosa* (*25, 26*). Reaction traces monitored at 386 nm were fit to a single exponential model and the rate constants for formation of the absorbing species were found to be proportional to the O_2 concentration (Fig. 1*B*). The linear plot of k_{obs} at 386 nm versus oxygen concentration yielded a second-order rate constant of $k = 2.97 \pm 0.06 \times 10^4\ M^{-1}\ s^{-1}$ (Fig. 1*C*). These data are consistent with a bimolecular reaction between the reduced flavin bound to ActVA and oxygen to form the C(4a)-FMN-OOH intermediate.

The C(4a)-FMN-OOH then slowly converted to FMN_{ox} with a half-life of about 1400 s and was complete by ~1 hour, as seen from the appearance of the two characteristic bands of the oxidized flavin at 370 and 445 nm (Fig. 1*A*). The absorbance changes at 445 nm (Fig. 1*B*) were found to be independent of oxygen concentration. These data, which are consistent with our previous results from experiments at 25 °C, clearly show that ActVA strongly stabilizes the C(4a)-FMN-OOH intermediate (*17, 24*). At the end of this slow decay of the intermediate, 10 μM FMN_{ox} was detected (ε_{445nm} = 13 $mM^{-1}\ cm^{-1}$), indicating that all of the initial FMN_{red} was quantitatively oxidized to FMN_{ox} by O_2. An ε value at 386 nm of 9.6 $mM^{-1}\ cm^{-1}$ for the C(4a)-FMN-OOH species could then be calculated.

Interestingly, when free FMN_{red} was mixed with an air-saturated ActVA solution in the stopped-flow apparatus, kinetic traces were the same as those obtained when a preformed ActVA·FMN_{red} complex was mixed with the same concentration of oxygen (data not shown). This implies that almost no spontaneous oxidation of free FMN_{red} by O_2 occurred, even though autoxidation of free FMN_{red} by O_2 is a reasonably fast process. For example, 40 μM FMN_{red} is oxidized by 240 μM O_2, final concentration, in an autocatalytic reaction with a $t_{1/2}$ ~0.5 s (*27, unpublished data*), and no detectable C(4a)-FMN-OOH species is produced (*28*). This result implies that binding of FMN_{red} to ActVA preceding the formation of the C(4a)-FMN-OOH species is fast and precludes any significant oxidation of free FMN_{red} by oxygen. These results explain and are in full agreement with our previous steady-state kinetics experiments (*24*).

Reaction of ActVA-FMN_{red} with O_2 and pyronaphthohydroquinone substrate. The reaction of O_2 with FMN_{red} bound to ActVA in the presence of its substrate, reduced dihydrokalafungin (DHK_{red}), was investigated by stopped-flow spectrophotometry. An anaerobic solution containing 80 μM of DHK_{red}, 20 μM of FMN_{red} and an excess of ActVA (50 μM, to ensure that most of the FMN_{red} was in complex with ActVA) was mixed with equal volumes of oxygenated Tris-HCl buffer solution containing various amounts of O_2. In Figure 2, the reported data were observed with a final O_2 concentration of

595 μM. The reaction was followed at : (i) 365 nm, a wavelength that is useful for monitoring the formation of the C(4a)-FMN-OOH intermediate species (*22, 29, 30*) and at which DHK_{red} contributes to the absorbance minimally; (ii) 445 nm to monitor the formation of FMN_{ox}; (iii) 520 nm to monitor the formation of the hydroxylated DHK_{ox} product (DHK_{ox}-OH) (*24*). In addition, fluorescence emission at 530 nm (excitation at 390 nm) was recorded in order to follow the formation of C(4a)-FMN-OH (hydroxy-FMN) and FMN_{ox} species. For many flavin-dependent hydroxylases, the C(4a)-FMN-OOH intermediate does not exhibit significant fluorescence emission upon excitation at 390 nm, whereas the C(4a)-FMN-OH species is often highly fluorescent (*22, 29, 31*). The absorbance values at the above mentioned wavelengths are plotted as a function of time in Fig. 2*A*. These data indicate that the reaction proceeds through at least four successive phases (Fig. 2*A*, Table 1). Each trace could be fitted by the sum of four exponential processes using a single set of rate constants for data at all wavelenghts.

The rate constant k_1 for phase 1 was directly dependent on O_2 concentration (data not shown), indicating a bimolecular reaction with O_2. No FMN_{ox} (445 nm trace) and almost no C(4a)-FMN-OH (fluorescence at 530 nm) were observed during this first phase. Thus, the bimolecular rate constant ($3.96 \pm 0.05 \times 10^4$ M^{-1} s^{-1}) determined from the increase in absorbance at 365 nm is clearly associated with the formation of the C(4a)-FMN-OOH intermediate. This rate constant is only slightly different from that determined in the absence of the DHK_{red} substrate (Fig. 1*C*, $2.97 \pm 0.06 \times 10^4$ M^{-1} s^{-1}). In the subsequent phases, k_2, k_3, and k_4, were found to be independent of O_2 concentration (data not shown), indicating that they did not involve direct reactions with O_2.

In phase 2, the appearance of fluorescence at 530 nm (with excitation at 390 nm) reached a maximum at ~2 sec reaction time, with a rate constant of 1.48 ± 0.15 s^{-1}. Although there is only a small decrease in absorbance at 365 nm in this phase, the fluorescence data clearly reflect the hydroxylation reaction. Therefore, the above data are consistent with the formation of the C(4a)-FMN-OH intermediate species in phase 2, implying that hydroxylation of the DHK_{red} substrate occurred during that phase. The trace at 520 nm does not show any increase in absorbance during this phase as might be expected for DHK_{ox}-OH. The immediate product is therefore most likely DHK_{red}-OH, which has very little absorbance or fluorescence (unpublished data), and is not expected to contribute significantly to the absorption and fluorescence data during phase 2.

Phase 3 is best indicated by the strong increase in absorbance at 445 nm characterized by a rate constant of 0.16 ± 0.02 s^{-1}. This was due to formation of FMN_{ox}, which is expected to arise from dehydration of the C(4a)-FMN-OH intermediate. The small decrease of fluorescence with an identical rate constant (0.16 ± 0.02 s^{-1}) likely reflects the smaller fluorescence quantum efficiency of FMN_{ox} (with excitation at 390 nm) as compared to that of C(4a)-FMN-OH, as has been shown for other flavin-dependent hydroxylases (*29*, *31*).

Finally, phase 4 was mainly characterized by a slow increase of absorbance at 520 and 450 nm (0.013 ± 0.002 s^{-1}), which most likely represents the oxidation by O_2 of the hydroquinone, DHK_{red}-OH, into the quinone, DHK_{ox}-OH. This conclusion was also consistent with the spectrum recorded 200 s after mixing (Fig. 2*B*) that has an additional band extending to 600 nm. This spectrum is similar to that of a mixture of ~10 μM FMN_{ox} and ~10 μM DHK_{ox}-OH; the latter spectrum was presented in our previous work (*24*). Oxidation of hydroquinones and their derivatives such as DHK_{red} by O_2 appears to proceed through an autocatalytic mechanism with phases that are only partially dependent on the concentration of O_2 (*28*, *32*, *33*). This is also the case for the reaction of O_2 with DHK_{red}, which becomes oxidized in an autocatalytic process with very little O_2-dependence (data not shown).

The kinetic path of hydroxylation of DHK_{red} catalyzed by ActVA is summarized in Scheme 2. One interesting feature of this reaction is that the formation of the C(4a)-FMN-OOH intermediate, which in the presence of O_2 forms quickly after FMN_{red} is transferred to the monooxygenase, has very little dependence on the presence of the DHK_{red} substrate. This indicates that the substrate may bind after the hydroperoxide intermediate is formed, as observed with HPAH-C_2 (*22*), cyclohexanone monooxygenase (*34*), and microsomal flavin monooxygenase (*35*).

FMN_{red} transfer from ActVB to ActVA. Our previous investigations have shown that transfer of FMN_{red} from the reductase ActVB to the monooxygenase ActVA is thermodynamically favorable (*17*). To study the kinetics of this transfer reaction, we took advantage of the UV-visible signature of the ActVB·FMN_{red}·NAD^+ complex, which has a broad charge-transfer (C–T) band between 550 and 800 nm, as well as the formation of the C(a)-FMN-OOH intermediate that can be monitored at 380 nm. The C–T band originates from the interaction between NAD^+ and FMN_{red} in the ActVB active site (*14*). Our previous studies showed that, under anaerobic conditions, the addition of 1 equivalent of ActVA to the ActVB·FMN_{red}·NAD^+ complex resulted in total disappearance of the C-T band, implying that FMN_{red} was transferred from ActVB to ActVA (*17*).

In Fig. 3, an ActVB·FMN_{red}·NAD^+ complex (85, 20, and 20 µM, of each component, respectively) was anaerobically prepared by adding one equivalent of NADH to FMN_{ox} in the presence of ActVB. Then, the complex was mixed at 4°C with an equal volume of solution containing 45 µM ActVA and 600 µM O_2 in a stopped-flow spectrophotometer. The UV-visible difference spectra (spectra at various times minus the initial spectrum of the ActVB·FMN_{red}·NAD^+ complex; this mode of display makes it easier to view the overall changes) were recorded as a function of time from 7 to 150 ms after mixing. Addition of the aerobic solution of ActVA to the anaerobic solution containing ActVB·FMN_{red}·NAD^+ resulted in total disappearance of the broad C–T band within ~1 s, shown in Fig. 3A by the loss of absorbance between 440 and 700 nm. Simultaneously, an absorbance band centered at ~386 nm appeared, due to formation of the C(4a)-FMN-OOH species. The presence of an isobestic point at about 435 nm indicated an apparent direct conversion of the ActVB·FMN_{red}·NAD^+ complex to the C(4a)-FMN-OOH-ActVA complex.

Fig. 3*B* shows the kinetics of the absorbance changes at 386 nm (formation of C(4a)-FMN-OOH) and at 700 nm (disappearance of the C–T complex ActVB·NAD^+·FMN_{red}). Both traces could be fitted to a single exponential model with almost identical rate constants (k_{386nm} = 4.6 ± 0.1 s^{-1} and k_{700nm} = 5.0 ± 0.4 s^{-1}). It can be noted that this rate constant is smaller than that for the formation of the C(4a)-FMN-OOH·ActVA complex from the reaction of free FMN_{red} with O_2 in the presence of ActVA (k_{386nm} = 10.6 ± 0.1 s^{-1} for the reaction of 10 µM free FMN_{red} mixed with 22.5 µM ActVA and 300 µM O_2 final concentrations, Fig. 1 and data not shown). Although these results suggest that under the experimental conditions of Fig. 3 formation of the C(4a)-FMN-OOH intermediate is rate-limited by the release of FMN_{red} from ActVB, the relatively small difference in rates of these two processes tempers confidence in this conclusion. In order to further clarify the kinetics of dissociation of FMN_{red} from ActVB, we performed the experiments described below.

The HPAH-C_2 monooxygenase from *A. baumanii* is part of a two-component FMN-dependent monooxygenase similar to ActVA. Recently, it has been shown that under similar conditions to those used for ActVA in the experiment shown in Fig. 1, HPAH-C_2 monooxygenase binds free FMN_{red} and reacts with O_2 to form a C(4a)-FMN-OOH adduct very rapidly. The rate constant for binding FMN_{red} to HPAH-C_2 has been estimated to be > 10^7 M^{-1} s^{-1} and the ensuing reaction with O_2 occurs with a second-order rate constant of 1.1 10^6 M^{-1} s^{-1} (*22*). Thus, if HPAH-C_2 is reacted with free FMN_{red} in the presence of 300 µM O_2, the formation of the C(4a)-FMN-OOH intermediate will occur with a rate constant of ~330 s^{-1}, a value about 30 times greater than that reported for ActVA. Substitution of HPAH-C_2 for ActVA in an experiment such as that in Fig. 3 would clearly distinguish whether the release of FMN_{red} from ActVB is rate limiting. The experiment shown in Fig. 3 was repeated in the presence of HPAH-C_2 monooxygenase (25 µM, final concentration) in place of ActVA. As reported for the experiment with ActVA (Fig. 3), the ActVB·FMN_{red}·NAD^+ complex disappeared in parallel with the formation of the C(4a)-FMN-OOH intermediate (data not shown). The kinetics of the absorbance changes at 386 nm (formation of the C(4a)-FMN-OOH species) and at 700 nm (disappearance of the C–T complex ActVB·NAD^+·FMN_{red}) could be fitted to a single exponential model, with rate constants (Table 2, k_{386nm} = 4.7 ± 0.1 s^{-1} and k_{700nm} = 3.8 ± 0.1 s^{-1}) nearly identical to those obtained with ActVA (Table 2). These data are consistent with the limiting step for the transfer

of FMN_{red} from ActVB to the monooxygenase component being the release of FMN_{red} from the $ActVB{\cdot}NAD^+{\cdot}FMN_{red}$ complex.

Menadione and DCPIP are two redox dyes known to react very rapidly with reduced free flavin (*36*). When free FMN_{red} is mixed with two equivalents of either one of these oxidized dyes, the FMN_{red} becomes nearly fully oxidized during the dead time of the stopped-flow experiment (implying that $k_{ox} > 300\ s^{-1}$, Table 2). However, when $ActVB{\cdot}FMN_{red}{\cdot}NAD^+$ was mixed with either DCPIP or menadione under anaerobic conditions, the FMN_{red} was oxidized with rate constants of $6.2 \pm 0.1\ s^{-1}$ and $6.1 \pm 0.1\ s^{-1}$ for DCPIP and menadione, respectively (Table 2). In addition, the C–T complex (measured at 700 nm) disappeared with rate constants ($6.5 \pm 0.1\ s^{-1}$ and $6.3 \pm 0.1\ s^{-1}$ for DCPIP and menadione respectively, Table 2). These rate constants are more than 50-fold smaller than those obtained when free FMN_{red} reacted with these dyes (Table 2). As shown in Table 2, the rates of disruption of the charge-transfer complex obtained in the presence of the monooxygenases ActVA or HPAH-C_2 and with the two dyes were almost identical. These results suggest that the rate of oxidation of the $ActVB{\cdot}NAD^+{\cdot}FMN_{red}$ complex by the dyes as well as by the oxygenases is likely to be primarily limited by the release of FMN_{red} from the complex. The slightly greater rates obtained with the dyes compared to those obtained with the two oxygenases can be explained by the dyes reacting with the FMN_{red} before it is fully released from ActVB, whereas the C(4a)-FMN-OOH species can only form after FMN_{red} is completely released and transferred to the oxygenases.

Altogether, these data demonstrate that the formation of the C(4a)-FMN-OOH intermediate with the monooxygenases ActVA and HPAH-C_2 is limited by the release of FMN_{red} from the $ActVB{\cdot}NAD^+{\cdot}FMN_{red}$ complex followed by its transfer to the monooxygenase.

Inhibition of FMN_{red} transfer by NAD^+. Previous steady-state kinetics studies had shown that during the ActVB-catalyzed reaction ($FMN_{ox} + NADH \rightarrow FMN_{red} + NAD^+$) the release of the NAD^+ product occurs before that of FMN_{red} (*14*). We tested whether the presence of NAD^+ influences the transfer of FMN_{red} from the $ActVB{\cdot}NAD^+{\cdot}FMN_{red}$ complex to the monooxygenase by carrying out experiments similar to those described in the previous section with various concentrations of NAD^+. In these experiments HPAH-C_2 was used in place of ActVA because, as mentioned earlier, HPAH-C_2 forms C(4a)-FMN-OOH very rapidly (*22*). Therefore, under these conditions, the formation of the C(4a)-FMN-OOH species provides a convenient and reliable coupled assay for monitoring the release of FMN_{red} from ActVB.

As shown in Fig. 4, the $ActVB{\cdot}FMN_{red}{\cdot}NAD^+$ complex (235, 40, and 40 µM of the respective components), was anaerobically mixed with equal volumes of solutions containing various amounts of NAD^+. After 5 s (to allow the NAD^+ binding to come to equilibrium), this solution was mixed with an equal volume of an aerobic solution of HPAH-C_2 (50 µM HPAH-C_2 and 255 µM O_2), and the absorbance values at 386 and 700 nm of the final mixture were followed as a function of time (Figs. 4*A* and 4*B* respectively). Addition of increasing amounts of NAD^+ resulted in decreases of the rates of both the loss of the C–T complex (700 nm) and the formation of C(4a)-FMN-OOH (386 nm). For a given NAD^+ concentration, traces at both 386 and 700 nm could be fitted with a single exponential function with almost identical rate constants (Figs. 4*A* and 4*B*). As shown in Fig. 4*C*, a plot of the rate constants obtained from the traces at 386 and 700 nm versus NAD^+ concentration indicated that the presence of an excess of NAD^+ could totally inhibit the transfer of FMN_{red} from ActVB to HPAH-C_2 as well as the formation of the C(4a)-FMN-OOH species. The IC_{50} concentration for inhibition by NAD^+ was determined to be ~40 µM.

DISCUSSION

In this work, we have carried out a detailed kinetic study of the reaction of the two-component FMN-dependent monooxygenase, ActVA-ActVB from *Streptomyces coelicolor*, by stopped-flow spectrophotometric methods in order to test our earlier propositions on the reaction mechanism of ActVA-ActVB system (*17*, *24*) and to gain insights into its mechanism of regulation. Recent characterization of several members of the two-component flavin-dependent monooxygenase family has revealed similarities to but also some specific

differences from the well-studied single component flavoprotein monooxygenase family, such as *p*-hydroxybenzoate hydroxylase. In both types of systems, the monooxygenase activates the oxygen molecule by forming a C(4a)-flavin hydroperoxide intermediate that delivers an oxygen atom to the substrate. In contrast to the single component hydroxylases, the reduction of the flavin in the two-component flavin-dependent monooxygenase systems is catalyzed by a separate NADH oxidoreductase and the resultant reduced flavin must then be delivered to the oxygenase. Thus, the mechanism by which the reduced flavin cofactor is transferred from the reductase to the monooxygenase in the presence of O_2 represents one of the most challenging aspects of these systems. Here we have presented several experiments that elucidate the essential features of the mechanism of transfer of FMN_{red} between ActVB and ActVA. Compared with the few studies recently published on other two-component FMN-dependent monooxygenase systems, our results highlight a unique property of the ActVA-ActVB system, namely that the overall hydroxylase reaction is partially limited by the release of FMN_{red} from the reductase, and this release is regulated by the dissociation rate of the charge transfer complex between NAD^+ and FMN_{red}. Large concentrations of NAD^+, a product of the flavin reductase reaction, can greatly reduce the rate of FMN_{red} release. Moreover, we show that no complexes between ActVB and ActVA are required for efficient transfer of FMN_{red} between the two.

At first, we studied the monooxygenase-dependent reaction in the absence of the reductase component ActVB and under conditions where the ActVA·FMN_{red}·DHK_{red} complex was formed before it reacts with O_2. We showed that the hydroxylation mechanism proceeds with the participation of two different reaction intermediates, a C(4a)-FMN-OOH that precedes, and a C(4a)-FMN-OH species that accompanies the formation of the reaction product, DHK_{red}-OH (Fig. 2). The C(4a)-FMN-OOH intermediate, characterized by a typical single absorbance band centered at 386 nm, results from the bimolecular reaction of the ActVA·FMN_{red} complex with O_2. This step occurs with a rate constant of ~4 x 10^4 M^{-1} s^{-1}, essentially independent of the presence of the DHK_{red} substrate. We note that in the monooxygenase HPAH-C_2 component from *A baumannii*, when C_2 in complex with FMN_{red} and its substrate, 4-hydroxyphenylacetate (at 2 mM), is mixed with O_2, the rate of formation of the C(4a)-FMN-OOH intermediate is significantly smaller than when the substrate is absent or when the HPAH-C_2-FMN_{red} complex is mixed with a solution containing 4-hydroxyphenylacetate and O_2. Thus, it could be concluded that normally FMN_{red} binds first, then O_2 reacts to form the C(4a)-FMN-OOH, and finally, 4-hydroxyphenylacetic acid binds before hydroxylation takes place (*22*). For ActVA, with the substrate concentrations used in this study (0, 10 and 40 μM DHK_{red}, Fig. 1*C*, data not shown and Fig. 2*A*, respectively), no effect of DHK_{red} on the kinetics of the reaction could be observed. However, because of the limited availability of the DHK substrate (it is not commercially available and has limited solubility), we could not determine if such an effect occurs with higher concentrations of DHK_{red}, and therefore we do not know the preferred order of binding.

In the presence of DHK_{red}, the C(4a)-FMN-OOH intermediate in the ActVA active site converted to a C(4a)-FMN-OH species, with a rate constant of 1.48 s^{-1}. Formation of the C(4a)-FMN-OH species results from transfer of the distal oxygen of C(4a)-FMN-OOH to the substrate, so that hydroxylation of DHK_{red} to give DHK_{red}-OH almost certainly occurred during that phase. In the subsequent step, the dehydration of the C(4a)-FMN-OH intermediate to form FMN_{ox} was observed at a rate of 0.16 s^{-1} (Fig. 2 and Scheme 2).

The mechanism of DHK_{red} hydroxylation catalyzed by ActVA with participation of the two reaction intermediates demonstrated in this study (Scheme 2) appears to be quite similar to that recently determined for the HPAH-C_2 component from *A. baumannii* (*22*), as well as that proposed for several single component hydroxylases (*1, 18, 25, 28, 34, 35*). These results reveal that, despite a rather low sequence identity between ActVA and HPAH-C_2 (23 % identities), the monooxygenase components in the two-component flavin-dependent monooxygenase family use similar chemical mechanisms of hydroxylation.

In the absence of the substrate, the C(4a)-FMN-OOH intermediate forms rapidly (~3 x 10^4 M^{-1} s^{-1}) and is remarkably stable, as previously observed (*17, 24*), and thus slowly converts to FMN_{ox} (and probably H_2O_2) with a

half-life of ~1400 s. Formation of the hydroperoxide intermediate in the absence of substrate has also been observed for other members of the two-component flavin-dependant monooxygenase family, such as styrene monooxygenase from *Pseudomonas Putida* S12 (*37*), the HPAH-C_2 monooxygenase from *A. baumannii* (*22*) and bacterial luciferase (*38*). The recently solved X-ray structure of the HPAH-C_2 monooxygenase from *A. baumannii* in complex with FMN_{red} has revealed the presence of a cavity adjacent to the isoalloxazine ring of the flavin molecule that is appropriate for harbouring the oxygen atoms of the C(4a)-FMN-OOH intermediate (*39*). It was proposed that this cavity provides a solvent-free environment that prevents rapid breakdown of the peroxide intermediate, thus accounting for its stability. In ActVA, one might expect an even more sequestered environment around the C(4a)-position of the flavin, because the C(4a)-FMN-OOH intermediate is about 75-fold more stable than in HPAH-C_2 (half-life of 1400 s for ActVA and 18 s for HPAH-C_2, this work and (*22*)). A sequence alignment between these two proteins shows that in HPAH-C_2 the amino-acid residues involved in the formation of the cavity near the C(4a)-position of the flavin are not totally conserved in ActVA. Presumably, these differences are responsible for the variations in stability of the peroxide intermediates.

Because in two-component FMN-dependent monooxygenases the reduction of the flavin takes place in a protein separate from the monooxygenase, FMN_{red} must be transferred from the reductase to the monooxygenase in the presence of O_2 without being oxidized unproductively. This represents a rather challenging process. Autooxidation of FMN_{red} can be toxic to the cell because it produces the harmful $O_2^{\bullet-}$ and H_2O_2 species, and in addition, is wasteful of reducing equivalents by effectively decoupling the reduction of the flavin by NADH and the hydroxylation reaction. We have previously shown that in the case of the ActVA-ActVB system such decoupling does not occur to any measurable extent (*17, 24*), but the mechanism by which it is avoided was not documented. The results of the present study now provide some insight into this mechanism.

i) First, we showed that ActVA binds free FMN_{red} rapidly enough to prevent autooxidation of free FMN_{red}. Bruice and colleagues have determined that the initial rate of reaction of O_2 with free FMN_{red} occurs at 250 M^{-1} s^{-1} (*40*). Thus, in the presence of 200 µM O_2, this initial rate should be 0.05 s^{-1} and, even considering the ensuing autocatalytic oxidation process known for such reactions (*28, 32, 40*), very little net oxidation of free FMN_{red} will occur within the first 100 ms (*27*). The formation of the C(4a)-FMN-OOH intermediate (Fig. 1*C*) occurs at a rate of 5.9 s^{-1} ($t_{1/2}$ ~100 ms) whether FMN_{red} is premixed with ActVA before or after mixing with O_2. Because the binding of FMN_{red} to ActVA does not limit the rate of formation of the rate of formation of the C(4a)-FMN-OOH, binding must occur at a rate ≥ 60 s^{-1} ($t_{1/2} \leq 10$ ms), and thus will be complete before any appreciable autooxidation of flavin happens.

This fast binding of FMN_{red} to ActVA represents one of the key catalytic features of these systems where reduction of the flavin and activation of O_2 occur in two different polypeptides. In addition to avoid uncoupling reactions during FMN_{red} transfer, this fast binding of FMN_{red} to ActVA also allows the rationalization of why the formation of a complex between the reductase and the monooxygenase is not required for efficient oxygenation reactions.

ii) Second, we demonstrated that dissociation of NAD^+ from ActVB limits the release and transfer of FMN_{red} from the reductase ActVB to the monooxygenase ActVA. We showed that the dissociation of FMN_{red} from ActVB is tightly regulated by NAD^+, which must dissociate before FMN_{red} can be released in the rate limiting step. A stable C–T complex between FMN_{red} and NAD^+ within the active site of ActVB limits the dissociation rate of NAD^+. Accordingly, when the kinetics of the FMN_{red} transfer between ActVB and ActVA was studied in the presence of increasing amounts of NAD^+, a strong inhibition of the transfer of FMN_{red} to ActVA was observed. An IC_{50} for NAD^+ of 40 µM was determined, and the inhibition of the FMN_{red} transfer was almost complete in the presence of 1 mM NAD^+. Therefore in *S. coelicolor*, ActVB, the reductase component can act as a regulatory component of the monooxygenase activity by controlling the transfer of the FMN_{red} cofactor to the monooxygenase.

Earlier steady-state kinetics studies showing that during ActVB catalysis, after the reduction of FMN_{ox} by NADH via hydride transfer, the NAD^+ product is released before FMN_{red} from the active site, in an ordered sequential mechanism (*14*). This confirms the notion that FMN_{red} cannot dissociate from the ActVB active site when NAD^+ is bound. Then, according to Le Chatelier's principle, an increase of NAD^+ concentration is likely to promote the formation of ActVB·FMN_{red}·NAD^+ complex and thereby prevent the release of free FMN_{red}. This is consistent with the experiments presented above showing strong inhibition of the transfer of FMN_{red} from ActVB to ActVA by NAD^+.

Control of the monooxygenase activity by NAD^+ is unprecedented in the two-component flavin dependent monooxygenase family. However, in most studies, high concentrations of NAD^+ were not present in reaction mixtures. Furthermore, few systems share with ActVB the observable rather stable $flavin_{red}$·NAD^+ charge-transfer complex. PheA2, the reductase of a two-component phenol hydroxylase from *Bacillus thermoglucosidasius*, is one such example *(3)*, and it is possible that similar control of the activity by NAD^+ also occurs in that case. Crystal structures show that NAD^+ binds directly over the FAD_{red} in a position that is ideal for charge-transfer interactions *(41)*. Recently, it was proposed that the activity of the monooxygenase component in the *A. baumannii* system was limited by the transfer of FMN_{red} from the reductase, HPAH-C_1, to the monooxygenase, HPAH-C_2 *(27)*. Furthermore, HPA, the monooxygenase substrate, was shown to function as an effector of HPAH-C_1 for both FMN reduction and FMN_{red} release (*19, 27*). Thus, as in the case of the ActVA-ActVB system, HPAH-C_1, the reductase component, is likely to regulate the overall monooxygenase activity. However, in that case the effector is the substrate of the monooxygenase, HPA, whereas in ActVA-ActVB system it is NAD^+, the product of the reductase.

Interestingly, it was also previously suggested that the oxygenases of the ActVA-ActVB system (*24*) and the 4-hydroxyphenylacetate hydroxylase (*42*) systems could be endowed with a regulatory function with respect to their reductases. In the absence of substrate, ActVA, traps free FMN_{red} and converts it to a stable C(4a)-FMN-OOH intermediate. The consequence is that the cellular content of free FMN can become depleted, resulting in a shut-down of the reductase component activity. As highlighted by this work, the regulatory role of ActVB that is dependent on the intracellular concentration of NAD^+ adds another important piece to the puzzle of the dynamic regulation of the ActVA-ActVB monooxygenase activity in a cellular context. It might allow coordination of the production of the DHK_{red}-OH (and consequently the formation of the actinorhodin) to the energetic state of the cell, as determined by the NADH/NAD^+ ratio. When this ratio is low in cells depleted of NADH, the FMN_{red} would remain bound to the reductase component, preventing further oxidation of NADH and leading to the arrest of the hydroxylase activity.

It therefore seems that for the two-component monooxygenase systems there is a mutual regulation mechanism allowing the interpretation of different cellular signals for rapidly tuning the activities of each partner according to the demand and the status of the cell. In the case of the ActVA-ActVB system, ActVA could be perceived as the sensor of the intracellular concentration of DHK, whereas ActVB could be a sensor of the cellular energetic level indicated the NADH/NAD^+ ratio.

Finally, the results on the two-component flavin-dependent systems from *A. baumannii* (*27*) and *S. coelicolor* (*17, 24 and this work*) reveal that free diffusion of FMN_{red} between two components in the presence of O_2 can be very efficient for supporting monooxygenation reactions. It is clear that single component flavin-dependent monooxygenases can coordinate and carry out both reduction of the flavin and hydroxylation of substrates. Therefore, the advantage of a system using separate reductases and a monooxygenases might be questioned. Because flavin reduction and oxygen-dependent reactions have very different requirements that are difficult to fulfil with a single polypeptide, dividing the tasks by using two different enzymes is a reasonable strategy to alleviate this challenge. In the case of the single component flavoprotein hydroxylases, coordinated dynamics between two different conformations that effectively provides two "active sites" has been shown to be important for dealing with this challenge (*1, 18*). This coordination is usually linked to the

substrate of the enzyme, so that adaptation to new substrates to trigger this dynamic dance of catalysis can be quite involved and complicated. Therefore, the two-component monooxygenase organization might represent an evolutionary advantage for quickly adapting to the metabolism of new substrates. The reductase and the monooxygenase polypeptides can acquire new complementary properties individually without modifying the structural requirements of the other component. This strategy more readily allows for variations to adapt to the hydroxylation of a broad range of substrates, as well as to different regulatory profiles. As pointed out above, even though the hydroxylation reactions occur with similar reaction mechanisms, the regulatory processes of the monooxygenase activity at the level of the reductase component in the case of the *A. baumannii* and *S. coelicolor* appear to be very different. Although such regulatory processes have not yet been explored for other two-component flavin monooxygenase systems, one might expect to find similar as well as new regulatory schemes for other systems. Consistent with this notion is the realization that two-component systems are continually being shown to be involved in the oxidation of an ever broader range of substrates.

REFERENCES

1. Entsch, B., Cole, L. J., and Ballou, D. P. (2005) *Arch Biochem Biophys* **433**, 297-311
2. Xun, L., and Sandvik, E. R. (2000) *Appl Environ Microbiol* **66**, 481-486
3. Kirchner, U., Westphal, A. H., Muller, R., and van Berkel, W. J. (2003) *J Biol Chem* **278**, 47545-47553
4. Beltrametti, F., Marconi, A. M., Bestetti, G., Colombo, C., Galli, E., Ruzzi, M., and Zennaro, E. (1997) *Appl Environ Microbiol* **63**, 2232-2239
5. Panke, S., Witholt, B., Schmid, A., and Wubbolts, M. G. (1998) *Appl Environ Microbiol* **64**, 2032-2043
6. Blanc, V., Lagneaux, D., Didier, P., Gil, P., Lacroix, P., and Crouzet, J. (1995) *J Bacteriol* **177**, 5206-5214
7. Thibaut, D., Ratet, N., Bisch, D., Faucher, D., Debussche, L., and Blanche, F. (1995) *J Bacteriol* **177**, 5199-5205
8. Eichhorn, E., van der Ploeg, J. R., and Leisinger, T. (1999) *J Biol Chem* **274**, 26639-26646
9. Xi, L., Squires, C. H., Monticello, D. J., and Childs, J. D. (1997) *Biochem Biophys Res Commun* **230**, 73-75
10. Chaiyen, P., Suadee, C., and Wilairat, P. (2001) *Eur J Biochem* **268**, 5550-5561
11. Caballero, J. L., Martinez, E., Malpartida, F., and Hopwood, D. A. (1991) *Mol Gen Genet* **230**, 401-412
12. Cole, S. P., Rudd, B. A., Hopwood, D. A., Chang, C. J., and Floss, H. G. (1987) *J Antibiot (Tokyo)* **40**, 340-347
13. Fernandez-Moreno, M. A., Martinez, E., Boto, L., Hopwood, D. A., and Malpartida, F. (1992) *J Biol Chem* **267**, 19278-19290
14. Filisetti, L., Fontecave, M., and Niviere, V. (2003) *J Biol Chem* **278**, 296-303
15. Kendrew, S. G., Harding, S. E., Hopwood, D. A., and Marsh, E. N. (1995) *J Biol Chem* **270**, 17339-17343
16. Parry, R. J., and Li, W. (1997) *J Biol Chem* **272**, 23303-23311
17. Valton, J., Filisetti, L., Fontecave, M., and Niviere, V. (2004) *J Biol Chem* **279**, 44362-44369
18. Ballou, D. P., Entsch, B., and Cole, L. J. (2005) *Biochem Biophys Res Commun* **338**, 590-598
19. Sucharitakul, J., Chaiyen, P., Entsch, B., and Ballou, D. P. (2005) *Biochemistry* **44**, 10434-10442
20. Fernandes, R. A., and Brückner, R. (2005) *Synlett*, 1281-1285
21. Tanaka, H., Minami-Kakinuma, S., and Omura, S. (1982) *J Antibiot (Tokyo)* **35**, 1565-1570
22. Sucharitakul, J., Chaiyen, P., Entsch, B., and Ballou, D. P. (2006) *J Biol Chem* **281**, 17044-17053
23. Patil, P. V., and Ballou, D. P. (2000) *Anal Biochem* **286**, 187-192

24. Valton, J., Fontecave, M., Douki, T., Kendrew, S. G., and Niviere, V. (2006) *J Biol Chem* **281**, 27-35
25. Entsch, B., and Ballou, D. P. (1989) *Biochim Biophys Acta* **999**, 313-322
26. Palfey, B. A., Ballou, D. P., and Massey, V. (1995) *Active Oxygen in Biochemistry*, Valentine, J. S., Foote, C. S., Greenberg, A., Liebman, J. F., ed., Blackie Academic and Professional, 37-83
27. Sucharitakul, J., Phongsak, T., Entsch, B., Svasti, J., Chaiyen, P., and Ballou, D. P. (2007) *Biochemistry* **46**, 8611-8623
28. Massey, V. (1994) *J Biol Chem* **269**, 22459-22462
29. Yeh, E., Cole, L. J., Barr, E. W., Bollinger, J. M., Jr., Ballou, D. P., and Walsh, C. T. (2006) *Biochemistry* **45**, 7904-7912
30. Ghisla, S., Entsch, B., Massey, V., and Husein, M. (1977) *Eur J Biochem* **76**, 139-148
31. Moran, G. R., Entsch, B., Palfey, B. A., and Ballou, D. P. (1997) *Biochemistry* **36**, 7548-7556
32. Massey, V., Palmer, G., and Ballou, D. P. (1973) *Flavin and Flavoproteins*, Second International Symposium, King, T. E., Mason, H. S., and Morrison, M., ed., University Park Press, Baltimore, 25-49
33. Muller, F. (1987) *Free Radic Biol Med* **3**, 215-230
34. Sheng, D., Ballou, D. P., and Massey, V. (2001) *Biochemistry* **40**, 11156-11167
35. Beaty, N. B., and Ballou, D. P. (1981) *J Biol Chem* **256**, 4619-4625
36. Gibian, M. J., and Rynd, J. A. (1969) *Biochem Biophys Res Commun* **34**, 594-599
37. Kantz, A., Chin, F., Nallamothu, N., Nguyen, T., and Gassner, G. T. (2005) *Arch Biochem Biophys* **442**, 102-116
38. Abu-Soud, H., Mullins, L. S., Baldwin, T. O., and Raushel, F. M. (1992) *Biochemistry* **31**, 3807-3813
39. Alfieri, A., Fersini, F., Ruangchan, N., Prongjit, M., Chaiyen, P., and Mattevi, A. (2007) *Proc Natl Acad Sci U S A* **104**, 1177-1182
40. Bruice, T. C. (1984) *Isr J Chem* **24**, 54-61
41. van den Heuvel, R. H. H., Westphal, A. H., Heck, A. J. R., Walsh, M. A., Rovida, S., van Berkel, W. J. H., and Mattevi, A. (2004) *J Biol Chem* **279**, 12860-12867
42. Louie, T. M., Xie, X. S., and Xun, L. (2003) *Biochemistry* **42**, 7509-7517

FOOTNOTES

We thank Dr. Jeerus Sucharitakul for providing HPAH-C_2 from *Acinetobacter baumannii*, Prof. Dr. Reinhard Brückner and Dr. Rodney Fernandes for providing enantiopure (+)-Kalafungin, and L. David Arscott, Dr. Sumita Chakraborty and Dr. Mike Tarasev for fruitful discussions and technical assistance.

The abbreviations used are: C(4a)-FMN-OOH, FMN C(4a)-hydroperoxide; DHK_{ox}, dihydrokalafungin quinone form; DHK_{red}, dihydrokalafungin dihydroquinone form; DHK_{red}-OH hydroxylated dihydrokalafungin dihydroquinone; HPAH-C_2, 4-hydroxyphenylacetate 3-hydroxylase; HPAH-C_1, 4-hydroxyphenylacetate 3-hydroxylase reductase component; DCPIP, 2,6-dichlorophenolindophenol; PCA, protocatechuate; PCD, protocatechuate dioxygenase; C(4a)-FMN-OH, FMN C4(a)-hydroxy.

FIGURE LEGENDS

Figure 1. Reaction of ActVA·FMN_{red} with O_2 at pH 7.4, 4°C. A solution containing ActVA (50 µM) and FMN_{red} (20 µM) in anaerobic 50 mM Tris-HCl buffer, was mixed in the stopped-flow instrument with an equal volume of oxygenated 50 mM Tris-HCl buffer, (O_2 was 595 µM after mixing). A. UV-visible spectra of the mixture (from the bottom to the top at 450 nm) recorded before and 5, 62, 180, 300, 480, 660, 930, 1200, 1860, 2400, and 4320 s after mixing. B. Same protocol, but performed in the presence of various concentrations of O_2 (60, 125, 299 and 595 µM after mixing). The absorbance traces at 386 nm as a function of time (dotted lines) are shown for each O_2 concentration. Solid lines are fits to a single exponential model. (♦) is the absorbance trace at 445 nm in the presence of 595 µM O_2, indicating the appearance of oxidized FMN. C. Plot of the pseudo first-order rate constants determined from the traces recorded at 386 nm shown in Fig. 1B as a function of O_2 concentration**.** A second-order rate constant of $2.97 \pm 0.06\ 10^4\ M^{-1}\ s^{-1}$ for the formation of the ActVA·C(4a)-FMN-OOH species was calculated from the slope of the straight line.

Figure 2. Reaction of the ActVA·FMN_{red} complex with DHK_{red} and O_2. An anaerobic solution containing ActVA (50 µM), FMN_{ox} (20 µM), DHK_{ox} (80 µM), in 50 mM Tris-HCl buffer, pH 7.4, containing 10 % glycerol, was incubated for 20 minutes in the dark in the presence of PCA (50 µM), PCD (0.12 unit.mL), EDTA (10 mM), and 5-deazaflavin (60 nM). The mixture was illuminated by white light until the FMN and DHK were fully reduced (5-10 s), and then was mixed at 4°C in the stopped-flow instrument with an equal volume of the same buffer containing oxygen (595 µM O_2). A. Traces of fluorescence (λ_{exc}=390 nm and λ_{em}> 530 nm) (□) and of absorbance at 365 (◇), 445 (○) and 520 nm (∇) vs. time (dotted lines). The four reaction phases are demarcated by dashed vertical lines. The dependence of each individual phase on oxygen is indicated at the top of the figure. Solid lines are fits for multi-exponential models, with $k_1 = 3.96 \pm 0.05 \times 10^4\ M^{-1}\ s^{-1}$, $k_2 = 1.48 \pm 0.15\ s^{-1}$, $k_3 = 0.25 \pm 0.03\ s^{-1}$ for the 365 nm trace, $k_3 = 0.16 \pm 0.02\ s^{-1}$ and $k_4 = 0.013 \pm 0.002\ s^{-1}$ for the 445 and 520 nm traces and $k_2 = 1.48 \pm 0.15\ s^{-1}$, $k_3 = 0.16 \pm 0.02\ s^{-1}$, and $k_4 = 0.013 \pm 0.002\ s^{-1}$ for the fluorescence trace. For the sake of clarity, all the traces are shifted to be zero intensity at 5 ms. B. Same protocol, but monitored with a diode array spectrophotometer. Spectra shown are recorded vs. anaerobic buffer (○), and at 150 ms (△), 2 s (□), 200 s (◇) after the addition of O_2.

Figure 3. FMN_{red} transfer from ActVB to ActVA and formation of C(4a)-FMN-OOH. An anaerobic solution containing ActVB (85 µM), NAD^+ (20 µM), FMN_{red} (20 µM), PCA (50 µM), and PCD (0.12 unit.mL) was mixed in the stopped-flow instrument with an equal volume of oxygenated buffer containing ActVA (45 µM) and O_2 (600 µM) at 4°C. Both solutions were in 50 mM Tris-HCl buffer, pH 7.4, containing 10 % glycerol. Concentrations given are those before mixing. A. UV-visible difference spectra of the mixture (spectrum at a given time minus the initial spectrum) recorded from 7 ms to 1.5 s with a diode array spectrophotometer. The arrows indicate the direction of spectral evolution as a function of time. B. Absorbance traces (solid line) at 386 nm and 700 nm as a function of time. The smooth lines are fits to a single exponential model. Rate constants: $k_{386nm} = 4.6 \pm 0.1\ s^{-1}$ and $k_{700nm} = 5.0 \pm 0.4\ s^{-1}$ were determined.

Figure 4. Inhibition of FMN_{red} transfer from ActVB to HPAH-C_2 by NAD^+. An anaerobic buffered solution containing ActVB (235 µM), NAD^+ (40 µM), FMN_{red} (40 µM), PCA (50 µM), PCD (0.12 unit.mL), was first mixed with an equal volume of the same buffer containing various concentrations of free NAD^+ (0 to 5000 µM). After 5 s this solution was mixed with an equal volume of the same buffer solution containing HPAH-C_2 (50 µM) and O_2 (255 µM). All concentrations given are those before mixing. The buffer used was 50 mM Tris-HCl, pH 7.4, containing 10 % glycerol, 4°C. The absorbance traces at 700 nm (A) and 386 nm (B), for each concentration of NAD^+ (10, 40, 125, 325, 625 and 1250 µM, concentrations after the second mix) are plotted as a function of time. The solid and smooth lines are fits for a single exponential model. C. The rate constants $k_{obs\ 386\ nm}$ (○) and $k_{obs\ 700\ nm}$ (•) obtained from Figs. 4A and 4B are plotted as a function of NAD^+ concentration. The concentration of NAD^+ required to inhibit the rate of FMN_{red} transfer from ActVB to HPAH-C_2 by 50 % is 40 µM.

Table 1. Rate constants determined from multi-exponential fits for the 365, 445, and 520 nm absorbance and fluorescence traces of Fig. 2A. The k_1 (M^{-1} s^{-1}) value is directly proportional to O_2 concentration, whereas k_2, k_3, and k_4 (s^{-1}) values are independent of O_2 concentration.

Trace	k_1	k_2	k_3	k_4
365 nm	$3.96 \pm 0.05 \times 10^4$ M^{-1} s^{-1}	1.48 ± 0.15 s^{-1}	0.25 ± 0.03 s^{-1}	/
445 nm	/	/	0.16 ± 0.02 s^{-1}	0.013 ± 0.002 s^{-1}
520 nm	/	/	0.16 ± 0.02 s^{-1}	0.013 ± 0.002 s^{-1}
Fluorescence at 530 nm	/	1.48 ± 0.15 s^{-1}	0.16 ± 0.02 s^{-1}	0.013 ± 0.002 s^{-1}

Table 2. Reactions of free FMN_{red} and ActVB·FMN_{red}·NAD^+ with ActVA, HPAH-C_2, DCPIP, and menadione. Anaerobic solutions containing either ActVB (85 µM), NAD^+ (20 µM) and FMN_{red} (20 µM) or solely FMN_{red} (20 µM), as well as PCA (25 µM), and PCD (0.12 unit. mL^{-1}) in 50 mM Tris-HCl buffer, pH 7.4, containing 10 % glycerol, were mixed with an equal volume of the same buffer containing either ActVA (45 µM) and O_2 (600 µM), HPAH-C_2 from *Acinetobacter baumannii* (45 µM), and O_2 (600 µM), oxidized DCPIP (20 µM), or menadione (40 µM). All reactions were carried out at 4°C and the concentrations given are those after mixing. The absorbance traces at 386 and 700 nm were recorded as a function of time (as in Fig. 3) and were fit with a single exponential model. The rate constants (s^{-1}) obtained from the traces at 386 (a), 450 (b) and 700 nm (c) are given below.

	ActVA + O_2	HPAH-C_2 + O_2	ActVA, no O_2	DCPIP	Menadione
Free FMN_{red}	10.6 ± 0.1^a	$330^{a, (22)}$	/	$> 300^b$	$> 300^b$
ActVB·FMN_{red}·NAD^+	4.6 ± 0.1^a 5.0 ± 0.4^c	4.7 ± 0.1^a 3.8 ± 0.1^c	6.6 ± 0.9^c	6.2 ± 0.1^b 6.5 ± 0.1^c	6.1 ± 0.1^b 6.3 ± 0.1^c

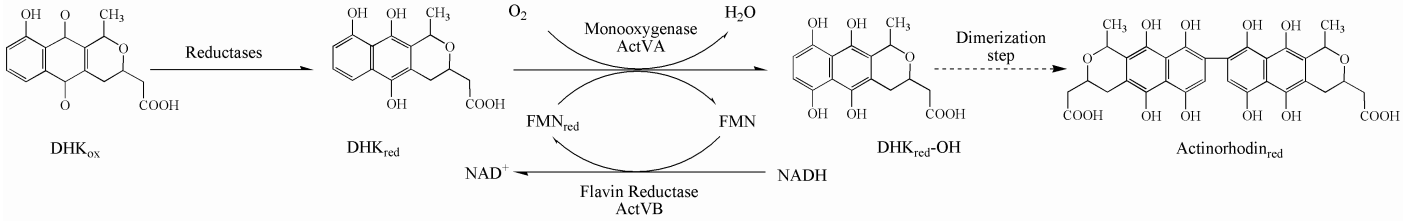

Scheme 1. Hydroxylation reaction catalyzed by the two-component ActVA-ActVB system from *Streptomyces coelicolor*. The reductase ActVB provides FMN_{red} to the monooxygenase ActVA. The ActVA substrate (DHK_{red}), is the dihydroquinone form of dihydrokalafungin (DHK_{ox}). Formation of Actinorhodin requires an additional DHK_{red}-OH dimerization step that has not been characterized *(24)*.

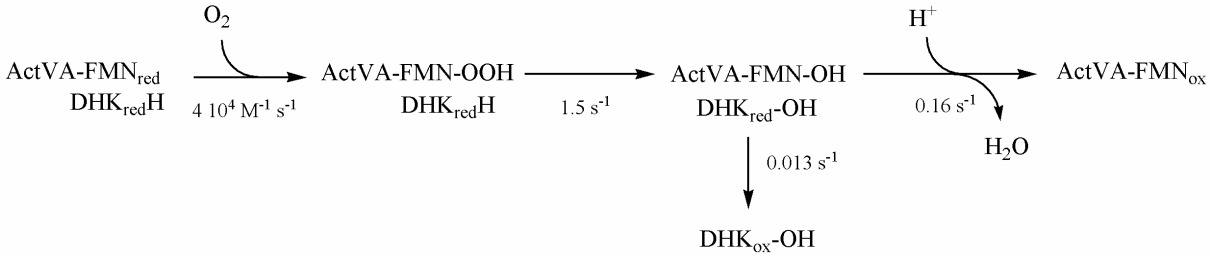

Scheme 2. Minimal catalytic scheme of the ActVA-catalyzed hydroxylation of DHK_{red}.

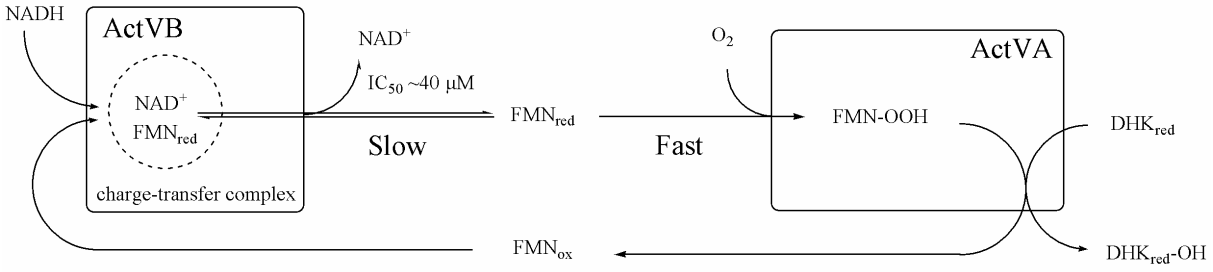

Scheme 3. Scheme of FMN_{red} transfer from reductase, ActVB, to the hydroxylase, ActVA. NAD^+ controls the release of FMN_{red} from ActVB and therefore acts as a regulator of the hydroxylase activity.

Figure 1

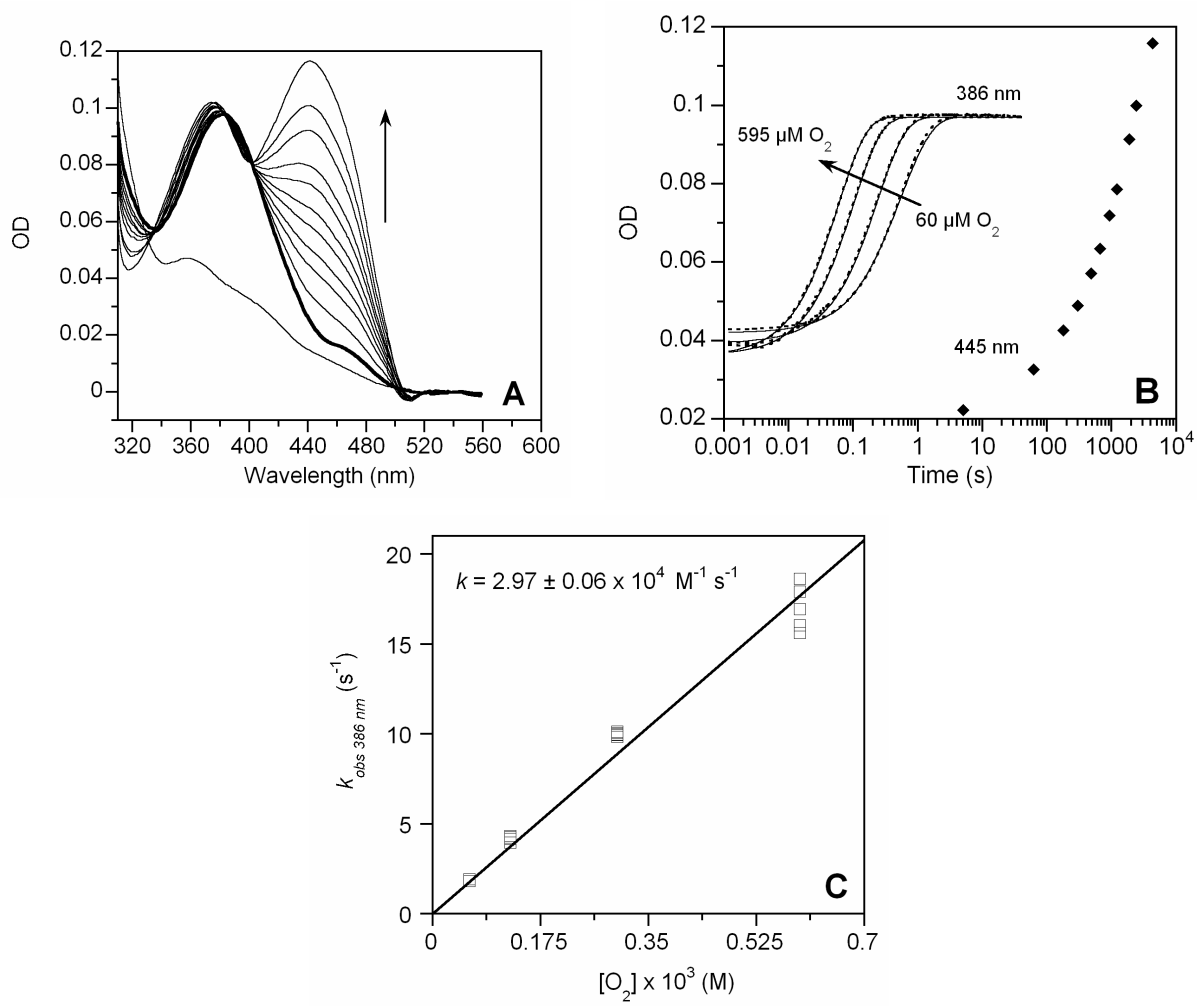
A
OD
Wavelength (nm)
B
386 nm
595 µM O2
60 µM O2
445 nm
OD
Time (s)
C
k = 2.97 ± 0.06 x 10^4 M^-1 s^-1
k obs 386 nm (s^-1)
[O2] x 10^3 (M)

Figure 2

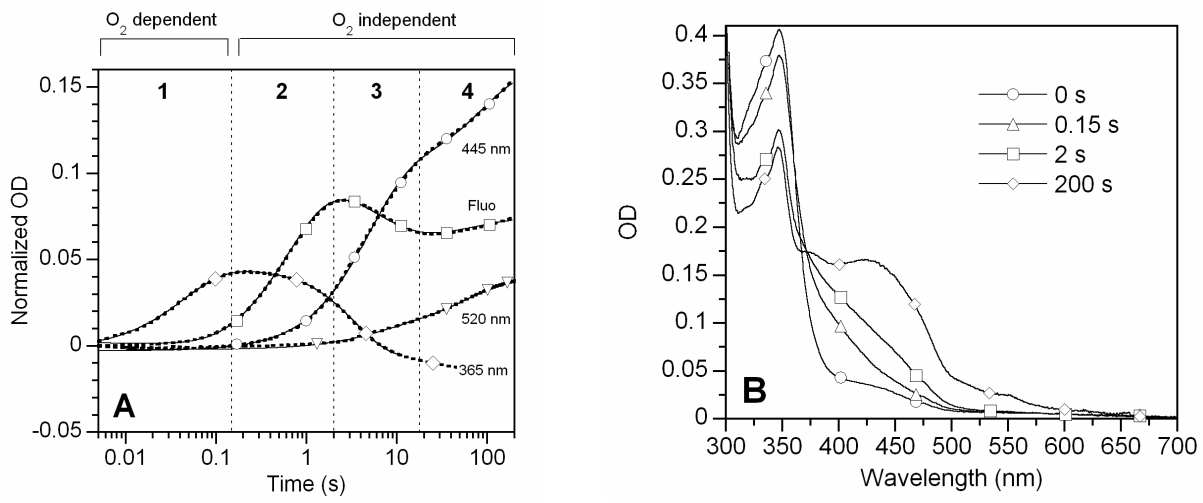
O2 dependent
O2 independent
1
2
3
4
445 nm
Fluo
520 nm
365 nm
A
Normalized OD
Time (s)
B
OD
Wavelength (nm)
0 s
0.15 s
2 s
200 s

Figure 3

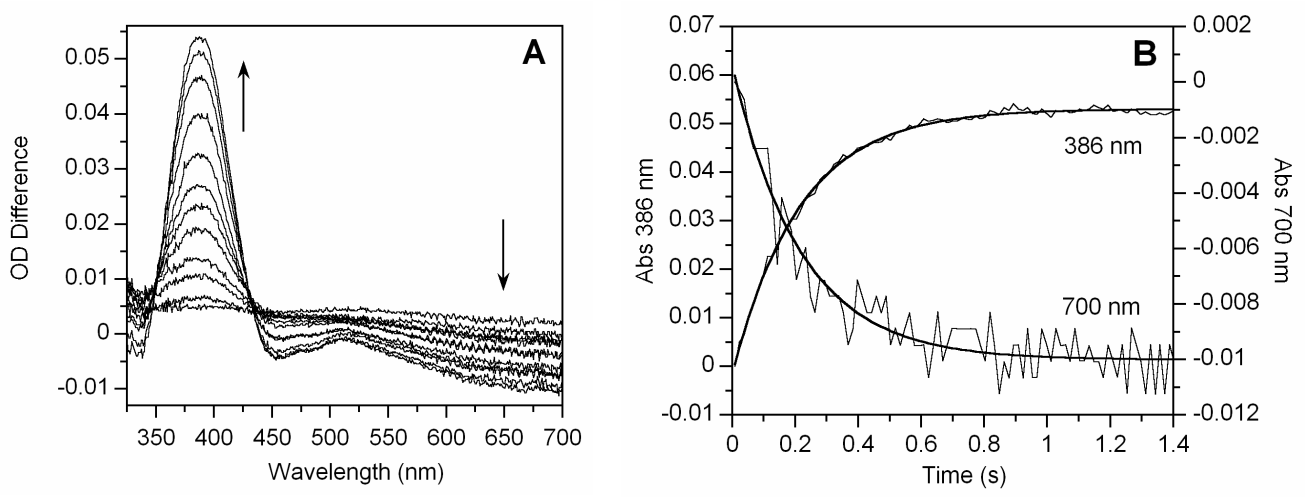
A
OD Difference
0.05
0.04
0.03
0.02
0.01
0
-0.01
350
400
450
500
550
600
650
700
Wavelength (nm)
B
Abs 386 nm
Abs 700 nm
386 nm
700 nm
0.07
0.06
0.05
0.04
0.03
0.02
0.01
0
-0.01
0.002
0
-0.002
-0.004
-0.006
-0.008
-0.01
-0.012
0
0.2
0.4
0.6
0.8
1
1.2
1.4
Time (s)

Figure 4

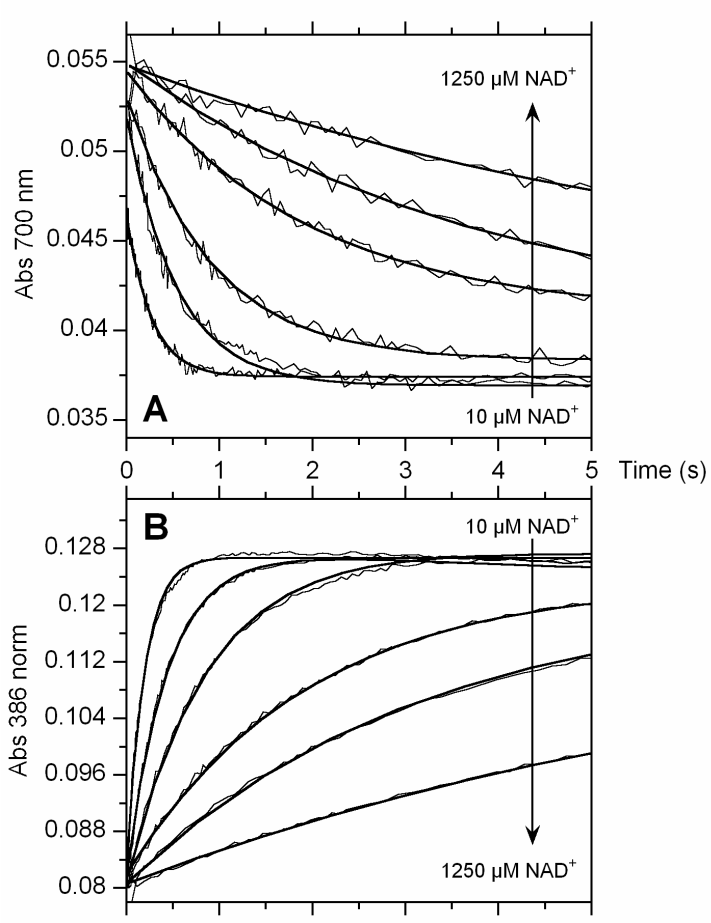
A
1250 µM NAD+
10 µM NAD+
Abs 700 nm
Time (s)
B
10 µM NAD+
1250 µM NAD+
Abs 386 norm

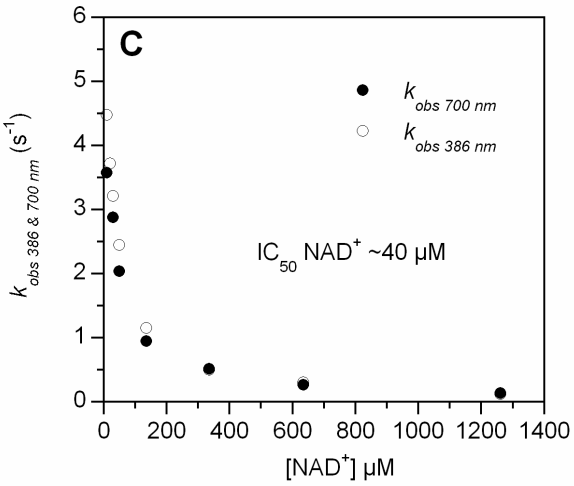
C
$k_{obs\ 700\ nm}$
$k_{obs\ 386\ nm}$
IC_{50} NAD^+ ~40 µM
$k_{obs\ 386\ \&\ 700\ nm}$ (s^{-1})
[NAD^+] µM